Reflection of Ultrasonic Wave on the Substrate-Ice Layer-Air Interface: The Role of Roughness Parameters

LU Qingwen[1], *WANG Yuan*[1], *WANG Jingxin*[1], *WANG Yan*[1], *ZHU Chunling*[1,2*], *ZHU Chengxiang*[1], *LI Bin*[3], *REN Zhanpeng*[3]

1. College of Aerospace Engineering, Nanjing University of Aeronautics and Astronautics, Nanjing 210016, P. R. China; 2. State Key Laboratory of Mechanics and Control for Aerospace Structures, Nanjing University of Aeronautics and Astronautics, Nanjing 210016, P. R. China; 3. National Key Laboratory of Strength and Structural Integrity, China Aircraft Strength Research Institute, Xi'an 710065, P. R. China

(Received 5 November 2025; revised 16 January 2026; accepted 30 January 2026)

Abstract: Ice accretion on transmission lines poses a severe threat to the safety of power grids. To achieve early icing warning and online ice thickness measurement, it is necessary to consider the effect of the rough ice layer on ultrasonic echo signals during the early icing stage. This study applied a sinusoidal equivalent roughness model to simplify the ice layer profile, and used PZFlex to numerically analyze the effects of the rough structure scale on the ultrasonic pulse-echo signals. The reflection coefficient of the ice-air layer interface was introduced to characterize small-scale roughness. It is found that the attenuation of pulse-echo signals is dominant by the height of rough structure. As the roughness upper ice layer increases, the interface reflection coefficient gradually decreases. When the roughness exceeds the critical value, the reflection coefficient shows independent with roughness. As the threshold of reflection coefficient is set as 0.25, the effective measurement range of roughness under different center frequencies of excitation signal sources is determined. The relationship between the reflection coefficient and roughness upper ice layer is established, enabling the quantitative identification of rough ice layer using the ultrasonic pulse-echo technique. The research can provide a technical basis for the accurate measurement of ice thickness above transmission lines.

Key words: ice accretion on cables; ice roughness measurement; ultrasonic measurement technology; reflection coefficient

CLC number: TM75 **Document code:** A **Article ID:** 1005-1120(2026)02-0275-11

0 Introduction

Ice accretion on overhead lines directly threatens the stability of power grids and induces issues such as grid overload[1], line galloping[2], tower inclination[3], and insulator pollution flashover[4], which severely endangers the safety of power systems. Traditional mechanical de-icing systems lack accurate operation instructions; therefore, ice monitoring on transmission lines is crucial for preventing grid freezing disasters.

Currently, the ice accretion state monitoring technologies for high-voltage transmission lines are mainly categorized into the weighting method, tension-inclination method, optical fiber method, image method and simulated conductor method, etc[5]. Most of the aforementioned detection methods are based on the principle of electromagnetic measurement, which are susceptible to interference and unable to achieve long-distance online quantitative measurement of ice thickness or identification of ice types.

To improve the stability of online ice accretion monitoring for lines, ultrasonic detection is introduced for transmission lines icing. Previous studies

*Corresponding author, E-mail address: clzhu@nuaa.edu.cn.

How to cite this article: LU Qingwen, WANG Yuan, WANG Jingxin, et al. Reflection of ultrasonic wave on the substrate-ice layer-air interface: The role of roughness parameters[J]. Transactions of Nanjing University of Aeronautics and Astronautics, 2026, 43(2): 275-285.

http://dx.doi.org/10.16356/j.1005-1120.2026.02.008

have demonstrated the feasibility of using ultrasonic waves to detect cable icing[6]. In 2023, Yang et al.[7] proposed a method for detecting the ice thickness of 10 kV overhead transmission lines using ultrasonic waves, with the relative error of the measured ice thickness being less than 10%. Liu et al.[8] proposed a method for direct ultrasonic detection of ice thickness on distribution lines using steel rods to simulate conductors, where the maximum error was less than 10%. However, the smooth surface of the simulated conductors fails to reflect the actual icing state.

The two aforementioned studies introduced ultrasonic detection technology for cable icing detection. However, for ultrasonic detection, the attenuation of echo signals is particularly pronounced when encountering different ice layer roughnesses. Therefore, identifying the surface roughness of ice deposits warrants special attention. To date, ice roughness measurement techniques are divided into contact and non-contact types. Traditional contact methods[9], e.g., ice tracing and hot wax molding[10], are inefficient, error-prone, and damage ice structures, leading to incomplete roughness data. Non-contact methods like close-range photogrammetry[11-13] or laser scanning[14-16] reconstruct ice profiles: The former uses multiple cameras but has large errors due to camera placement, glaze ice transparency and complex data processing; the latter is widely used for high-precision, multi-scale measurement[15] but requires developer due to optical properties of ice, leading to difficulty of real-time measurement.

In summary, current techniques struggle with initial icing stage and transient roughness measurement. Ultrasonic pulse-echo (UPE) technology shows advantages, which uses echo parameter changes to measure thickness and properties of ice[17]. Jr Hansman et al.[18] noted that ice surface properties affected ultrasonic signals, and Liu et al.[19] reported that frequency-dependent attenuation characterized glaze and rime ice. However, it is harder to measure ice surface roughness than ice thickness/density due to its spatiotemporal variations[20]. Relative research focus on the application of UPE on roughness surface measurement in other fields. Okajima et al.[21] estimated planar Manning roughness coefficients using the peak-to-peak value of reflected ultrasonic pulses. Ma et al.[22] developed an ultrasonic reflection coefficient phase spectrum technique to measure coating interface roughness (6.2—12.7 μm). Hériveaux et al.[23] used a sinusoidal equivalent model to characterize bone-implant interface roughness via quantitative ultrasound. The results indicate that both of soft tissue thickness and interface roughness attenuate ultrasonic reflection coefficient. These studies confirm that surface roughness reduces ultrasonic interface reflection coefficients, which is beneficial to support UPE for measuring roughness upper ice layer of transmission lines.

Up to now, UPE technology has been initially applied in the field of aircraft icing[24], but there have been no reports on its application in the icing monitoring of transmission lines, especially in the quantitative characterization of surface roughness. There is still a lack of detailed research on the influence of the roughness upper ice layers on the attenuation of ultrasonic signals.

Within the range of actual roughness ice on transmission lines, this study numerically analyzed the attenuation of echo signals caused by the rough structure between air-ice layer interface. Determining the attenuation of echo signals caused by roughness parameters provides a basis for selecting transducer frequency parameters in experimental measurements. Another approach involves simulating equivalent simplified real ice roughness to reduce experimental costs, thereby obtaining the relationship between a wide range of ice roughness values and ultrasonic echo parameters, which guides ultrasonic identification of ice surface roughness. This paper used a sinusoidal equivalent model to describe the ice layer shape. The change of surface roughness is adjusted by the amplitude height and period of the sinusoidal function. Ultrasonic echo signals under multi-frequency excitation signals and different surface roughness are obtained through numerical simulation. The reflection coefficient affected by the ice layer shape is introduced to characterize ice roughness at different scales. The relationship between the effective identification range of roughness upper

ice layer and the frequency of the excitation signal is established.

1 Methods and Theories

1.1 Establishment of a simulation model for ice layers

As a powerful professional tool in acoustics, PZFlex software is specifically developed for piezoelectric and ultrasonic applications. The software adopts an explicit finite element algorithm, which is suitable for simulating piezoelectricity, ultrasonic wave propagation, and long-range wave propagation.

To study the influence of roughness at different scales on the attenuation of ultrasonic pulse-echo signals, the models and simulations of roughness ice are solved via PZFlex in this paper. The actual physical model is a complex-shaped cable with accreted ice. However, due to the small size of the applied transducer and the single-point measurement of the ice layer above its geometric center, the numerical model can be simplified to a 2D axisymmetric model. The process mainly involves model construction, mesh generation, material parameter configuration, and boundary conditions.

Due to the symmetry, a 2D axisymmetric model is used to reduce computational load. The model includes four parts: Pressure loading area, aluminum substrate, ice layer, and roughness. A non-structured mesh is used, with grid refinement for the ice layer interior; the rest adopts a 20 μm per grid, satisfying the requirement of at least 15 grids per wavelength. The upper surface of ice layer is set as a total reflection interface, while other boundaries are total absorption interfaces to reduce oscillation interference from secondary interface echoes. In the study, the transducer has a diameter of 6 mm. As the width of the load application area should be smaller than the model width, the width of both ice layer and substrate is set as 15 mm. The thickness of substrate, ice layer and load application area are 5, 1.6 and 0.5 mm, respectively. The rough profile on the ice surface is implemented via a sinusoidal function, with a single roughness element illustrated in the local enlarged view of Fig.1, where S_0, S_1 and S_2 represent the regions areas. The curve expression of roughness is expressed as

$$y = A \cdot \sin\left(\frac{2\pi}{T}x\right) \tag{1}$$

where A is the amplitude and T the period.

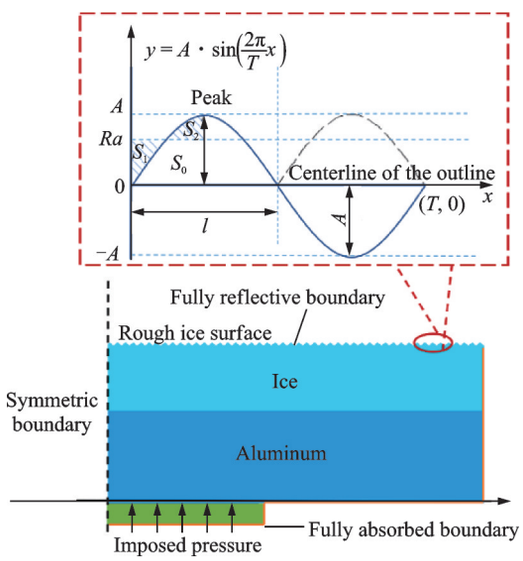

Fig.1 Schematic diagram of a simplified 2D symmetric finite element model for rough ice surfaces

The sinusoidal function is mainly described by two parameters: Amplitude A and period T. Roughness Ra is the arithmetic mean of the absolute values of profile deviations within the sampling length. Therefore, the roughness formula for this model is calculated as

$$Ra = \frac{1}{l}\int_0^l A \cdot \sin\left(\frac{2\pi}{T}x\right)\mathrm{d}x \tag{2}$$

For $l = T/2$, the calculated roughness Ra is expressed as

$$Ra = \frac{1}{l}\cdot\frac{AT}{\pi} = \frac{2A}{\pi} \tag{3}$$

According to above derivation, the average roughness Ra can be adjusted only by changing the peak value A in the sinusoidal function. Additionally, in all numerical cases, the average height of the surface roughness is regarded as the origin of the y-axil. It is assumed that all media have uniform and isotropic mechanical properties. The substrate material is 7075 aluminum alloy. The material properties[25-26] used in the simulation, with references, are presented in Table 1.

Table 1 Material attribute

Material	Mass density R/(kg•m^{-3})	Longitudinal velocity v_p/(m•s^{-1})	Shear velocity v_s/(m•s^{-1})
Ice	900	3 900	2 120
Aluminum	2 690	6 306	3 114

1.2 Finite element simulation

Dynamic equations were solved in the time domain via the PZFlex software. Post model construction and material assignment, the loading excitation signal were configured, and mesh generation was conducted. A Ricker wavelet served as the ultrasonic pulse excitation source.

To explore frequency-dependent roughness measurement ability, the simulation included excitation signals with center frequencies (f_c) of 3.2, 5.3, 7.5, 10, 12.8, and 15.5 MHz. During model establishment, the grid size is first determined by the signal's center frequency. A non-structured mesh is adopted, with a requirement of at least 15 elements per wavelength in the material. For grid size in the ice layer, the maximum center frequency is used to calculate the minimum wavelength, with the formula given below

$$\lambda_{min} = v_p / f_c \tag{4}$$

To explore the roughness-dependent echo signal, the roughness parameter was varied within the range of 0—1 000 μm in the study. For grid independence verification, the roughness size and the center frequency were fixed at 25 μm and 10 MHz, respectively. The grid size was evenly varied within the range of 1—10 μm. The verification results are presented in Fig.2 and Fig.3. The results indicate that when the grid size exceeds 5 μm, both the amplitude and phase of the echo signal are unstable. To ensure clarity, only echo signals for grid sizes of 1—5 μm are presented in Fig.2. Observing the ice layer echo signals, the amplitude fluctuation of the echo peak is blow 1% when the grid size is smaller than 4 μm, indicating that the echo peak at the air-ice interface is stable. Fig.3 presents the phase errors between the air-ice interface echo, substrate-ice interface echo, and the set thickness within the range of

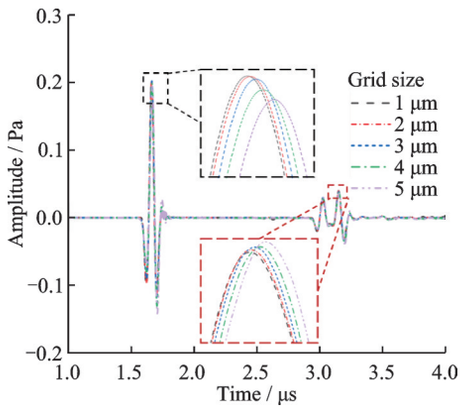

Fig.2 Variations in echo signals from the upper surface of the ice layer corresponding to different grid sizes

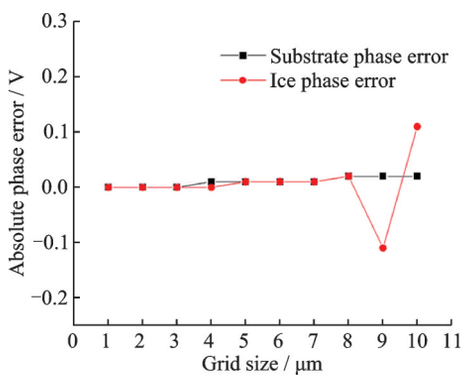

Fig.3 Phase deviation between rough ice layer height and original height corresponding to different grid sizes

1—10 μm. The results show that the peak time of the interface echo stabilizes when the grid size is below 3 μm. Considering the grid size for stability of echo signals, the grid size is set as 3 μm, to save computing loads and ensure the accuracy of numerical calculation results.

An un-structured rectangular mesh was adopted to reduce the number of meshes. For time-domain calculations, the maximum stable time step was set based on the minimum mesh size, as follows

$$\Delta t_{max} = d_{min} / c_p \tag{5}$$

where d_{min} denotes the minimum mesh side length, and c_p the maximum longitudinal wave speed in the model material.

The maximum stable time step is multiplied by a safety factor $k_0 = 0.8$ to obtain the maximum simulation timestep. Thus, the actual timestep t_s used in the simulation is given by

$$t_s = k_0 \cdot \Delta t_{max} = 0.38 \times 10^{-9}\,(\mathrm{s}) \tag{6}$$

Signal acquisition frequency is

$$f_0 = \frac{1}{t_s} \tag{7}$$

The sampling frequency meets the requirement of being greater than 10 times the center frequency. The simulation time is determined based on the transit time of the multi-layer material thickness, and is ultimately set to 5 μs through calculations.

From the derived formula for roughness, it can be seen that this expression is determined solely by the amplitude A. However, based on the inferred physical propagation of acoustic waves, variations in the period parameter T also induce changes in the model and consequently affect the echo signal. Therefore, the parameter $B=T/A$ was defined. With the amplitude A kept constant, simulations were conducted to investigate the effect of period T on the reflection coefficient of ultrasonic echo signals by varying period. The results are presented in Fig.4.

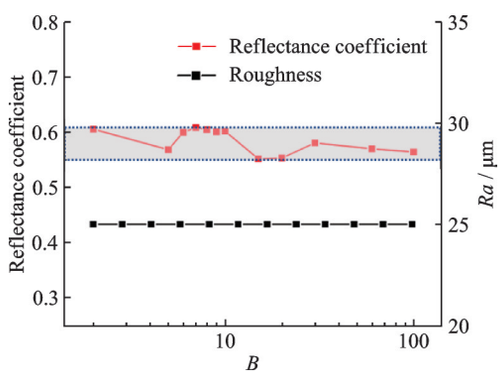

Fig.4 Effect of period variation of the sinusoidal function on roughness and reflection coefficient

Parameter B was assigned non-uniform values within the range of 0—100. It can be observed that parameter B exerts a certain influence on the echo signal. When $B>10$, the rough profile curve tends to approach a straight line, regraded as smooth surfaces. When $B<10$, variations in the period cause a relative error of 3% in the reflection coefficient. However, in actual measurements, ultrasonic detection acquires the average value of reflected echoes from the rough surface within the ice layer surface detection range. Thus, the influence of the period parameter is minimal. Furthermore, there is no need to decouple the effects of the period and amplitude on the echo characteristic parameters. In subsequent simulation cases, the period was set to $T=2A$, and the roughness value in the simulation was adjusted solely by varying the amplitude parameter. The settings of the ice layer roughness parameters are presented in Table 2.

Table 2 Settings for roughness in the simulation model

Serial number	Amplitude A/m	Cycle T	Roughness Ra/μm
1	0.00E+00	1.00E−03	0
2	3.93E−05	7.86E−05	25
3	7.85E−05	1.57E−04	50
4	1.18E−04	2.36E−04	75
5	1.57E−04	3.14E−04	100
6	2.36E−04	4.72E−04	150
7	3.14E−04	6.28E−04	200
8	3.93E−04	7.86E−04	250
9	4.71E−04	9.42E−04	300
10	5.5E−04	1.10E−03	350
11	6.29E−04	1.26E−03	400
12	7.07E−04	1.41E−03	450
13	7.85E−04	1.57E−03	500
14	8.64E−04	1.73E−03	550
15	9.43E−04	1.89E−03	600
16	1.10E−04	2.20E−03	700
17	1.26E−04	2.51E−03	800
18	1.41E−04	2.83E−03	900
19	1.57E−04	3.14E−03	1 000

1.3 Signal processing

In this study, ultrasonic echo signals from multi-layer medium interfaces with/without roughness were obtained via simulation calculations. The signals in the time domain were recorded and subsequently processed using MATLAB software. First, the Hilbert transform is applied to the echo signals, and the transformation results are presented in Fig.5. The solid line represents the original signal, while the dashed line denotes the signal envelope. Two gates #1 and #2 are set: Gate #1 covers the complete echo signal from the substrate-ice interface, while Gate #2 covers the complete echo signal from the ice-air interface. After envelope processing, the echo amplitudes $p_{A\text{-}I}$ (substrate-ice interface) and $p'_{I\text{-}a}$ (ice-air interface), along with their corresponding peak time t_1 and t_i, are identified with-

in the two gates, respectively. The real-time ice layer thickness is calculated using t_1 and t_i based on the ultrasonic transit time in the structure, which is used to compute ultrasonic attenuation in the ice. The substrate-ice interface echo amplitude $p_{A\text{-}I}$ is acquired. The echo amplitude $p_{I\text{-}a}$ for the ice-air interface with a smooth surface is calculated theoretically and numerically. In addition, under the same ice layer thickness, this study obtains the ice-air interface echo amplitude $p'_{I\text{-}a}$ when small-scale roughness elements exist on the ice surface. The formula for the ultrasonic reflection coefficient $R'_{I\text{-}a}$ at the ice-air interface with a rough structure is as follows

$$R'_{I\text{-}a} = \frac{p'_{I\text{-}a}}{p_{I\text{-}a}} \tag{8}$$

A comparison of simulation results between smooth ice surfaces and ice surfaces with rough profiles reveals that the waveform and phase of the echo signal at the substrate-ice interface are both affected by ice surface roughness. From the signal comparison in Fig.5, it is evident that when small-scale roughness elements exist on the ice surface, the echo amplitude at the ice-air interface decreases significantly, accompanied by phase delay. This conclusion is further confirmed by observing the shift in the peak points of the envelope. Thus, it is feasible to characterize the influence of roughness on ultrasonic echo signal by using the reflection coefficients.

Fig.6 illustrates the entire process of extracting characteristic parameters of ultrasonic echo signals. First, after determining the simulation model,

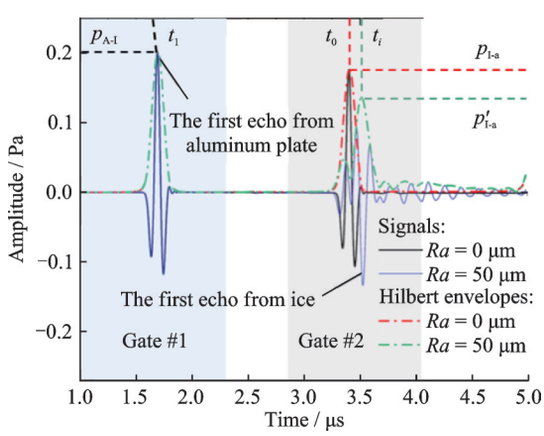

Fig.5 Schematic diagram of ultrasonic echo signal feature parameter extraction

roughness parameters are input. The reflection coefficient is then obtained by applying the aforementioned signal processing method and extracting amplitude parameters via envelope processing. By processing the original ultrasonic pulse-echo signals, the ultrasonic reflection coefficient at the ice-air interface was obtained. A corresponding relationship can be established between the reflection coefficient $R'_{I\text{-}a}$ and roughness parameters Ra. Therefore, the reflection coefficient can be used to calculate and predict the surface roughness of the ice layer.

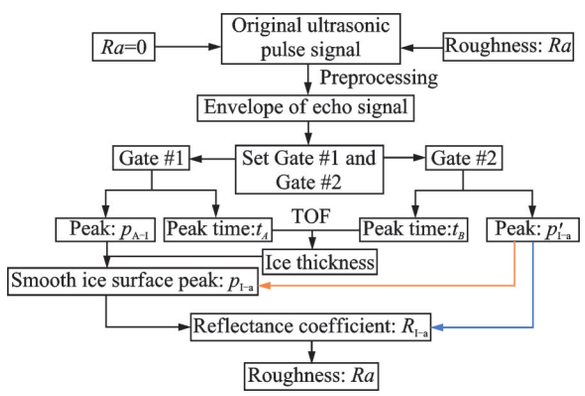

Fig.6 Flowchart for extraction of ultrasonic echo signal characteristic parameters

2 Results

2.1 Effect of surface roughness on ultrasonic signals

A series of numerical simulations were performed using the roughness parameters listed in Table 2. Glaze ice was selected as the representative ice type for simulations due to its hazard. The ultrasonic attenuation coefficient inside the simulated ice layer was set to 0.05 Np·mm^{-1}. The theoretical ice density was $\rho_{(i)}$ = 900 kg·m^{-3}, and the longitudinal wave speed was set to 3 900 m·s^{-1}. In a homogeneous solid, longitudinal waves propagate in a straight line with relatively low energy loss, producing a clear "emission-bottom echo" signal.

The original echo signals undergo preprocessing. After that, the ultrasonic echo envelopes, under different roughness conditions, are shown in Fig.7. The results show that with the increase of ice-air interface roughness, the echo amplitude decreas-

es irregularly and the arrival time of the peak shifts progressively later. For a perfectly smooth ice surface ($Ra = 0$), the echo amplitude at the ice-air interface was $p_{I\text{-}a} = 0.85$.

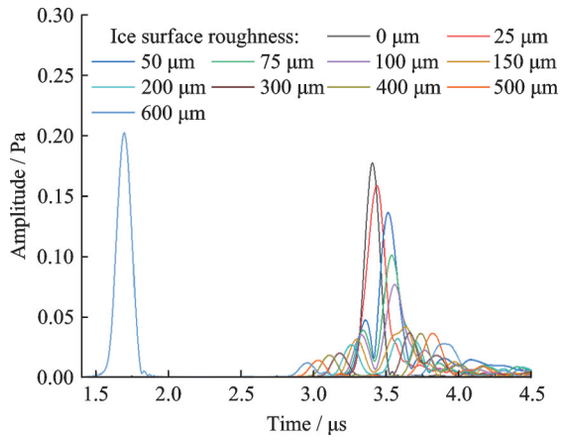

Fig.7 Influence of roughness on echo signals envelopes

Using the feature-extraction method described in Fig.6, the ultrasonic reflection coefficient of the ice-air interface was determined as a function of surface roughness, as shown in Fig.8. The simulation was performed at a center frequency of 7.5 MHz. The resulting curve agrees well with previously published results on effect of surface roughness[24].

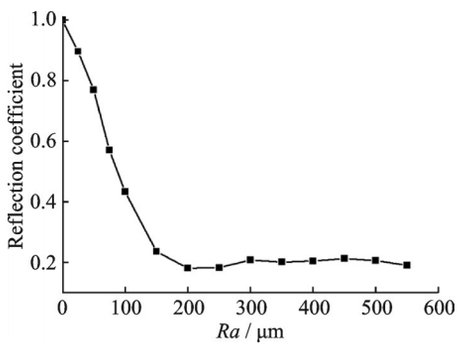

Fig.8 Reflection coefficient versus surface roughness

From Fig.8, when the surface roughness increases from 0 to 150 μm, the interface reflection coefficient $R'_{I\text{-}a}$ decreases from 1 to 0.23. For roughness values exceeding 150 μm, $R'_{I\text{-}a}$ stabilizes at about 0.2, showing a slight rise followed by a further decline. This behavior occurs because the sinusoidal roughness profile has alternating peaks and valleys. When the roughness becomes sufficiently large, the ultrasonic wave can resolve the height difference between the peaks and valleys, causing the ice-air interface echo to split into two distinct signals. Consequently, the reflection coefficient derived from the envelope analysis shows a slight increase before continuing to decline as roughness grows. For example, at a center frequency of 7.5 MHz, when the roughness is in the range of 0 — 100 μm, the echo signals are aliasing; once the roughness exceeds 100 μm, the echo signals become separated. The reflection coefficient decreases by as much as 80%, demonstrating that the ultrasonic reflection coefficient $R'_{I\text{-}a}$ is highly sensitive to roughness variations. Furthermore, the accuracy of using $R'_{I\text{-}a}$ as a quantitative indicator of surface roughness is confirmed.

2.2 Influence of center frequency on rough-surface echoes

The sensitivity of ultrasonic roughness detection varies with center frequency. To examine this effect under constant ice-layer thickness, the surface roughness was fixed at 100 μm while the center frequency of the ultrasonic excitation source was varied. The corresponding ice-air interface echo signals are shown in Fig.9. A higher excitation signal frequency results in a narrower bandwidth, higher detection sensitivity, and greater signal attenuation. Simulation results show that as the center frequency increases, the amplitude of the echo signal at the rough ice-air interface decreases monotonically. Furthermore, applying a high-frequency excitation source, two complete echo signals can be obtained, corresponding to the peak and trough points of the rough profile, respectively. This leads to greater attenuation of the high-frequency excitation signal under the same ice thickness and roughness conditions.

For ultrasonic pulse-echo detection signals with different center frequencies, there are significant differences in the identifiable scale range of material surface rough structures due to variations in their inherent wavelengths, attenuation coefficients, and detection sensitivity characteristics. High-frequency signals are more capable of identifying small-scale roughness values but suffer from greater energy at-

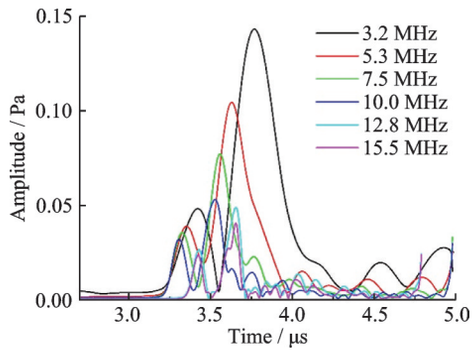

Fig.9 Effect of frequency variation on ultrasonic echoes from a rough ice surface

tenuation. However, low-frequency signals are suitable for larger-scale rough structures. These differences directly affect the measurement range and accuracy of rough features. To further investigate the capability of the ultrasonic pulse-echo technique for quantitative measurement of wide-range roughness, physical property measurements of ice layers with rough profiles were conducted under different center frequencies. The resulting reflection coefficients are presented in Fig.10. When $Ra = 50$ μm, the reflection coefficient decreases monotonically as the center frequency increases. When Ra increases to 200 μm, the reflection coefficient shows significant decrease once center frequencies exceeds 5.3 MHz. After the reflection coefficient falls below 0.25, interface echoes in the original signal waveform exhibit aliasing and low amplitude, making it impossible to distinguish from clutter. With a further increase in roughness size, the reflection coefficient shows no obvious change, and direct identification of roughness parameters via interface echo signals becomes infeasible in the situations.

The detection range of roughness measurement

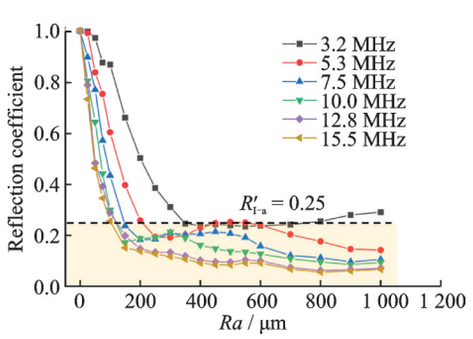

Fig.10 Ultrasonic reflection coefficient of the ice-air interface versus roughness

for different frequencies is shown in Fig.11.

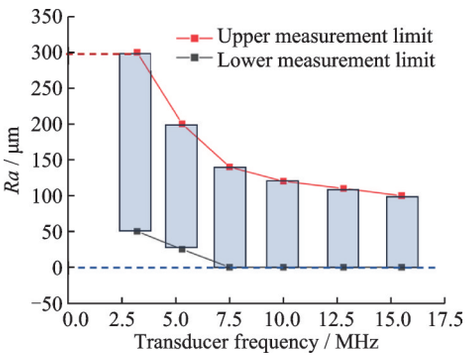

Fig.11 Roughness measurement range at different frequencies

In this study, a critical threshold of $R'_{f\text{-}a} = 0.25$ was used to distinguish the effective center frequency. As the center frequency increases, the upper limit of effective roughness identification decreases, while the accuracy of identifying small-scale roughness improves. The results show that as the transducer frequency increases, the upper limit of roughness measurement generally shows a decreasing trend. Meanwhile, the lower limit of roughness measurement gradually approaches 0 and stabilizes as the frequency increases. The result indicates that high-frequency transducers possess the capability to identify smaller-scale surface roughness features.

The higher the transducer frequency, the lower the upper limit of surface roughness can be accurately measured, while the stronger the ability to identify smaller rough structures. To quantitatively analyze the roughness identification range for different frequencies f, the fitted formula is as follows

$$Ra_{\max} = 607\exp(-f/2.9) + 99.36 \tag{9}$$

$$Ra_{\min} = \begin{cases} -11.63f + 87 & f \leqslant 7.5 \\ 0 & f > 7.5 \end{cases} \tag{10}$$

The influence laws of frequency and roughness on the ultrasonic reflection coefficient at the ice-air interface were refined via simulation calculations. The ice surface roughness range was determined. Then, the center frequency of the excitation source was selected. After extracting the characteristic parameters of the original signals, the corresponding relationship was obtained as shown in Fig.12.

The results in Fig.12 show that there is a

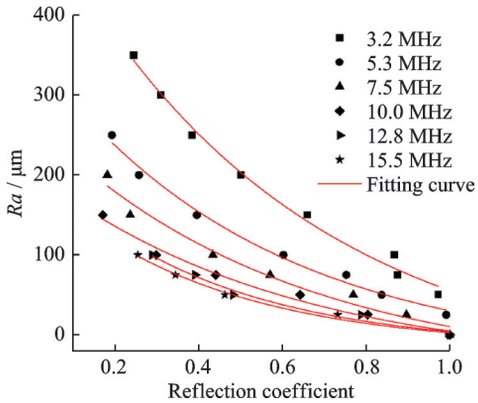

Fig.12 Relationship between ultrasonic reflection coefficient and roughness at the ice-air interface

monotonic relationship between roughness and reflection coefficient within a certain range. The red solid lines represent the fitting curves of roughness and ultrasonic reflection coefficient under different frequencies. The formula of the fitting curve is as follows

$$Ra = a_1 \cdot \exp(-R'_{I\text{-}a}/a_2) + a_3 \tag{11}$$

where a_1, a_2 and a_3 are the coefficients of the equation, and their variation relationships are expressed in Table 2.

Table 3 Equation coefficients

Frequency/MHz	a_1	a_2	a_3
3.2	603.7	0.59	−56.5
5.3	387.7	0.537	−30.3
7.5	319.3	0.592	−48.7
10.0	248.7	0.595	−41.88
12.8	232.6	0.413	−16.68
15.5	212.2	0.415	−16.48

The ultrasonic reflection coefficient $R'_{I\text{-}a}$ varies within the range of 0.2 — 1, corresponding to a roughness measurement range of 0 — 300 μm.

3 Conclusions

To investigate the reflection of ultrasonic echo signals on the substrate-ice layer-air interface, a novel multilayer model with a sinusoidal profile was introduced to simulate ultrasonic reflections from the roughness shape upper the ice layer. By adjusting the amplitude and period of the sinusoidal function, the available measure ranges of roughness ice surface at different center frequencies are quantitatively analyzed. The main findings are as follows.

(1) With the same center frequency, as the surface roughness increases, the amplitude of echo signals decreases and the phase of the peak point delays. The interface reflection coefficient gradually decreases until it shows independent of roughness and reflection coefficient.

(2) For small-scale roughness, as the center frequency increases, the both of the echo signal amplitude and the reflection coefficient also decrease monotonically. For large-scale roughness, increasing the center frequency leads to a significant decline in the reflection coefficient until it shows independent of the roughness and center frequency.

(3) As the center frequency increases, the upper limit for identifying effective roughness decreases, while the accuracy in identifying small-scale roughness increases.

(4) The reflection coefficient threshold is set as 0.25, the ice surface roughness value is quantitatively characterized through the interface echo signal, and the calculation formulas for roughness is fitted for various center frequency.

Applying ultra-pulse echo technology to monitor the transient icing process of transmission lines, it is important to select an appropriate transducer frequency for ice layers with different roughness to maximize the monitoring range. The research can provide a technical basis for the accurate measurement of ice thickness on transmission lines.

References

[1] RAMSANKAR V, LINCHUAN T, HAIYANG H, et al. An experimental study of dynamic icing process on an aluminum-conductor-steel-reinforced power cable with twisted outer strands[J]. Experimental Thermal and Fluid Science, 2023, 142: 110823.

[2] AN S H, WEI Z, TANG L, et al. Research on online monitoring and anti-dance technology of transmission line dance based on wide-area information transmission[J]. Applied Mathematics and Nonlinear Sciences, 2024, 9(1): 1-21.

[3] ZHANG G X, LIU M H, CHENG S C, et al. Research on transmission line tower tilting and foundation state monitoring technology based on multi-sensor cooperative detection and correction[J]. Energy Engineering: Journal of the Association of Energy Engineers, 2023, 121(1): 169-185.

[4] DENG Y, JIA Z D, ZHOU J, et al. Ice flashover performance and its characterization parameter of composite insulator with booster sheds[J]. IEEE Transactions on Dielectrics and Electrical Insulation: A Publication of the IEEE Dielectrics and Electrical Insulation Society, 2016, 23(2): 1021-1029.

[5] FENG C, YANG R, CAO X H, et al. Online monitoring and early warning technology for the status of earth wire for overhead line[J]. Journal of Physics: Conference Series, 2022, 2196(1): 012020.

[6] WU Y Q, LU P, ZHOU W S, et al. Ice monitoring of aluminum conductor steel-reinforced cables using guided waves[J]. Cold Regions Science and Technology, 2023, 210: 103835.

[7] YANG L, CHEN J, HAO Y P, et al. Experimental study on ultrasonic detection method of ice thickness for 10 kV overhead transmission lines[J]. IEEE Transactions on Instrumentation and Measurement, 2023, 72: 1-10.

[8] LIU Y L, XIAO X B, LI Y, et al. Ultrasonic direct detection method for ice thickness monitoring of distribution lines[C]//Proceedings of 2023 7th International Conference on Smart Grid and Smart Cities. Lanzhou, China: IEEE, 2023: 47-53.

[9] REEHORST A L, RICHTER G P. New methods and materials for molding and casting[C]//Proceedings of NASA Technical Memorandum. Washington, DC, USA: NASA, 1987: 15.

[10] ANDERSON D, SHIN J, ANDERSON D, et al. Characterization of ice roughness from simulated icing encounters[C]//Proceedings of the 35th Aerospace Sciences Meeting and Exhibit. Reno, NV, USA: AIAA, 1997: 52.

[11] SHIN J. Characteristics of surface roughness associated with leading-edge ice accretion[J]. Journal of Aircraft, 1996, 33: 316-321.

[12] COLLIER P, DIXON L, FONTANA D, et al. The use of close range photogrammetry for studying ice accretion on aerofoil[J]. The Photogramm Record, 1999, 16: 671-684.

[13] MCKNIGHT R, PALKO R, HUMES R. In-flight photogrammetric measurement of wing ice accretions[C]//Proceedings of the 24th Aerospace Sciences Meeting. Reno, NV, USA: AIAA, 1986: 483.

[14] MCCLAIN S T, VARGAS M M, TSAO J C. Ice roughness and thickness evolution on a swept NACA 0012 airfoil[C]//Proceedings of the 9th AIAA Atmospheric and Space Environments Conference. Denver, CO, USA: AIAA, 2017: 1.

[15] MCCLAIN S T, VARGAS M, TSAO J C, et al. Ice accretion roughness measurements and modeling[C]//Proceedings of the 7th European Conference for Aeronautics and Space Sciences. Milan, Italy: [s.n.], 2017: 555.

[16] NEUBAUER T, HASSLER W, PUFFING R. Ice shape roughness assessment based on a three-dimensional self-organizing map approach[C]//Proceedings of the AIAA Aviation 2020 Forum. [S.l.]: AIAA, 2020: 2805.

[17] COBBOLD R S. Foundations of biomedical ultrasound[M]. Oxford, United Kingdom: Oxford University Press, 2007.

[18] JR HANSMAN R J, KIRBY M, LICHTENFELTS F. Ultrasonic techniques for aircraft ice accretion measurement[C]//Proceedings of the Sensor and Measurements Techniques for Aeronautical Applications. Atlanta, GA, USA: AIAA, 1990: 4656.

[19] LIU Y, BOND L J, HU H. Ultrasonic-attenuation-based technique for ice characterization pertinent to aircraft icing phenomena[J]. AIAA Journal, 2017, 55: 1602-1609.

[20] MCCLAIN S T, VARGAS M, KREEGER R E, et al. A reevaluation of appendix C ice roughness using laser scanning[J]. SAE Technical Paper Series, 2015, 1: 2015-1-2098.

[21] OKAJIMA K, NAGAOKA S, ISLAM M R, et al. Development and testing of a surface roughness measurement device based on aerial ultrasonic reflections[J]. Paddy Water Environ, 2019, 18: 345-353.

[22] MA Z Y, LUO Z B, LIN L, et al. Quantitative characterization of the interfacial roughness and thickness of inhomogeneous coatings based on ultrasonic reflection coefficient phase spectrum[J]. NDT & E International, 2019, 102:16-25.

[23] HÉRIVEAUX Y, NGUYEN V H, BRAILOVSKI V, et al. Reflection of an ultrasonic wave on the bone-implant interface: Effect of the roughness parameters[J]. The Journal of Acoustical Society of America, 2019, 145(6): 3370.

[24] WANG Y, ZHANG Y, WANG Y, et al. Quantitative measurement method for ice roughness on an aircraft surface[J]. Aerospace, 2022, 9(12): 739.

[25] SENTHIL K, IQBAL M A, CHANDEL P S, et al. Study of the constitutive behavior of 7075-T651 aluminum alloy[J]. International Journal of Impact Engineering, 2017, 108: 171-190.

[26] PETRENKO V F, WHITWORTH R W. The physics of ice[M]. New York, NY, USA: Elsevier, 1999.

Authors

The first author Miss. **LU Qingwen** graduated with a bachelor's degree from Nanjing University of Aeronautics and Astronautics in 2023 and is currently pursuing a master's degree at the same institution. Her research focuses on ice monitoring and ultrasonic detection for power transmission cables, including the design and fabrication of ultrasonic transducers.

The corresponding author Prof. **ZHU Chunling** received the Ph. D. degree in mechanical engineering from Nanjing University of Aeronautics and Astronautics in 2007 and has engaged in the teaching and research of man-machine and environmental engineering for many years. Her research focuses on numerical simulation of aircraft icing, aircraft icing protection system technology, aircraft environmental control system design.

Author contributions Miss. LU **Qingwen** was responsible for drafting the core content and proofreading the manuscript to ensure textual accuracy and standardization. Dr. **WANG Yuan** assisted in organizing the research framework and selecting methodologies, participating in specialized discussions. Dr. **WANG Jingxin** and Dr. **WANG Yan** reviewed the article content, conducting scientific validation and verification to ensure the reliability of the findings. Prof. **ZHU Chunling** and Prof. **ZHU Chengxiang** provided research funding support. Mr. **LI Bin** and Mr. **REN Zhanpeng** managed the related project, coordinating resources and progress. All authors commented on the manuscript draft and approved the submission.

Competing interests The authors declare no competing inrests.

(Production Editor: ZHANG Huangqun)

基底-冰层-空气界面超声波反射:粗糙度参数的作用

陆庆文[1], 王 渊[1], 王敬鑫[1], 王 岩[1], 朱春玲[1,2], 朱程香[1], 李 斌[3], 任战鹏[3]

(1.南京航空航天大学航空学院,南京 210016,中国; 2.南京航空航天大学航空航天机械结构力学与控制国家重点实验室,南京 210016,中国; 3.中国飞机强度研究所强度与结构完整性全国重点实验室,西安 710065,中国)

摘要:输电线路结冰对电网安全构成严重威胁。为实现冰冻早期预警与在线冰厚测量,需考虑结冰初期粗糙冰层对超声回波信号的影响。本文采用正弦等效粗糙度模型简化冰层截面,运用PZFlex软件研究不同粗糙结构尺度对超声脉冲回波信号的影响。引入冰层-空气界面反射系数表征小尺度粗糙度。研究发现脉冲回波信号衰减主要受粗糙结构高度主导:随着冰层表面粗糙度增大,界面反射系数逐渐降低;当粗糙度超过临界值时,反射系数与粗糙度呈现无关性。以反射系数阈值0.25为基准,确定了不同中心频率激励信号下粗糙度的有效测量范围。建立了反射系数与粗糙冰层的关联,实现了利用超声脉冲回波技术对粗糙冰层进行定量识别。该研究为输电线路冰厚精确测量提供了技术依据。

关键词:线缆结冰;冰粗糙度测量;超声测量技术;反射系数

研究亮点:

1.引入超声换能器应用于线缆覆冰监测,通过仿真考虑冰表面粗糙度建立中心频率适用范围。

2.提出了基于界面声波反射系数定量表征冰层表面粗糙度方法。